

Subband structure comparison between n - and p -type double delta-doped GaAs quantum wells

I. Rodríguez-Vargas and L.M. Gaggero-Sager

Facultad de Ciencias, Universidad Autónoma del Estado de Morelos,
Av. Universidad 1001, Col. Chamilpa 62210 Cuernavaca, Morelos, México

Recibido el 26 de marzo de 2004; aceptado el 18 de agosto de 2004

We compute the electron level structure (n -type) and the hole subband structure (p -type) of double δ -doped GaAs (DDD) quantum wells, considering exchange effects. The Thomas-Fermi (TF), and Thomas-Fermi-Dirac (TFD) approximations have been applied in order to describe the bending of the conduction and valence band, respectively. The electron and the hole subband structure study indicates that exchange effects are more important in p -type DDD quantum wells than in n -type DDD. Also our results agree with the experimental data available.

Keywords: δ -doped quantum wells; electron and hole states; exchange effects.

Calculamos la estructura de niveles electrónicos (tipo- n), así como la de huecos (tipo- p) de pozos cuánticos δ -dopados dobles (DDD) en GaAs. Se han tomado en cuenta los efectos de intercambio en el estudio. Las aproximaciones de Thomas-Fermi (TF) y Thomas-Fermi-Dirac (TFD) han sido implementadas para describir el doblamiento de la banda de conducción y de valencia respectivamente. El estudio de la estructura de niveles electrónicos y de huecos revela que los efectos de muchos cuerpos son más importantes en los pozos DDD tipo- p que en los DDD tipo- n . De la misma manera nuestros resultados están en buen acuerdo con los datos experimentales disponibles.

Descriptores: Pozos δ -dopados; estructura electrónica; efectos de muchos cuerpos.

PACS: 73.30; 73.61; S5.11

1. Introduction

Nowadays, control and precision in growth and doping techniques allow the fabrication of systems where the impurity deposition is made with atomic resolution. A two dimensional electron (2DEG) or hole gas (2DHG) is formed if the impurity doping is made in an atomic plane (δ -doping technique), in such a way that the impurity density be enough to the effective Bohr radii between donors (n -type) or acceptors (p -type) overlapped. The forementioned situation was firstly proposed by Wood [1], and later brought it about by Ploog [2]; calling it a δ -doped quantum well n - or p -type, depending on whether we are working with donors or acceptors. The δ -doping technique is a useful tool in the fabrication of high power devices, and also for its possible technological applications in δ -FET [6,7], and ALD-FET [8] (where a δ -doped quantum well is used as a channel between the terminals of the transistor). There are several works in n - [3-8] and p -type [9-15] single δ -doped quantum wells (SDD).

Thomas-Fermi (TF) and Thomas-Fermi-Dirac (TFD) approximations have demonstrated to be useful tools in the theoretical treatment of δ -doped quantum wells [16-18]. The main advantage of these approximations is the possibility of obtaining an analytical solution to the Poisson equation. This allows us to avoid a long and troublesome self-consistent (SC) calculation. When the exchange effects are taken into account explicitly in the TF energy density functional, we are concerned with the TFD theory, *i.e.*, the generalization of the TF approximation. It is important to mention that the TFD theory is not applicable to describe the conduction band bending because the electron density $n(r)$ does not tend to

zero at infinity, a physical requirement in δ -doped quantum wells. The situation drastically changes when the carriers, responsible of the conduction, are holes, because the effective masses are negative and this avoids the algebraic origin of the above mentioned problems. As a consequence, the solution in this case is SC and satisfactory [18].

On the other hand, from the theoretical point of view, only a few works in DDD quantum wells are reported in Refs. 19 to 21. DDD quantum wells are very interesting as far as the device industry is concerned, since by the interlayer distance between wells and the impurity density varies, an improvement in the transport properties is achieved [22-24]. The present paper is devoted to the subband structure study in both n - and p -type DDD quantum wells. TF and TFD approximations are implemented in order to accomplish the level structure calculation. The many-body effects are also included to discern their relevance in the electron and hole level structure. A comparison between both systems is given, in the same way that our results are confronted versus the experimental data available.

Next section includes mathematical models followed with results, and finally with conclusions.

2. Mathematical Models

2.1. TF theory applied to n -type DDD GaAs quantum wells

Consider a GaAs matrix doped at atomic precision with a donor density n_{2D} of Si atoms in two of its planes, located at a certain distance l (the same impurity density is assumed

in both planes). The effective potential created by the 2DEG, and the ionized impurities causes a conduction band bending. We have used the TF theory in order to obtain an analytical solution for this potential [20].

$$V_H - \mu = -\frac{\alpha^2}{(\alpha|z + l/2| + z_{0n})^4}, \quad (1)$$

where $\alpha = 2/15\pi$, and $z_{0n} = (\alpha^3/\pi n_{2D})^{1/5}$.

But our survey is engaged in the study of exchange effects. The inclusion of the many-body effects is made through the Local Density Approximation (LDA), thereby the exchange potential is:

$$V_x(z) = -\frac{2}{\pi}(3\pi^2(a_0^*)^3 n(z))^{1/3} R_y^*, \quad (2)$$

where $a_0^* = \epsilon_r \hbar^2 / (e^2 m^*)$, and $R_y^* = e^2 / (2\epsilon_r a_0^*)$ are the effective Bohr radius, and the effective Rydberg constant. The rest of the equations presented in this subsection will be in effective units. The exchange potential can be written in terms of the Hartree potential, due to the relation between $n(z)$ and $V_H(z)$ [20]

$$V_x(z) = -\frac{2}{\pi}(\mu - V_H(z))^{1/2}. \quad (3)$$

Finally substituting (1) in (3) the total potential $V = V_H + V_x$ is

$$V(z) = -\frac{\alpha^2}{(\alpha|z + l/2| + z_{0n})^4} - \frac{2}{\pi} \frac{\alpha}{(\alpha|z + l/2| + z_{0n})^2}. \quad (4)$$

2.2. TFD theory in *p*-type DDD GaAs quantum wells

Again, a GaAs matrix has been considered, but instead of donor impurities, acceptor impurities are used to dope the system. Two planes of the host material are δ -doped (located at a distance l), with an impurity density p_{2D} . The acceptor impurities cause the presence of a 2DHG. Both ionized impurities, and 2DHG are responsible for the valence band bending, that in this case, we will describe it in terms of the TFD approximation. First of all, it is important to take notice of the hole ladders: the heavy (*hh*), the light (*lh*), and the split-off (*so*) holes. In our study, only *hh* and *lh* bands are taken into account, since the potential depth never exceeds the energy distance to the *so* band for the range of impurity density considered here ($p_{2D} \leq 1 \times 10^{13} \text{ cm}^{-2}$). This is shown in *p*-type SDD GaAs quantum wells [17].

The kinetic energy-density functional, the density functional associated to the interaction between 2DHG, the impurity planes, as well as the density functional concerning to the hole-hole interaction come as in Ref. 20. The exchange-energy functional is given by Ref. 18, adding the aforementioned terms we have E_{TFD} ,

$$E_{TFD} = \frac{3}{10m_{ed}} \int p(z) [3\pi^2 \hbar^3 p(z)]^{2/3} dz - \frac{e^2 \pi}{\epsilon_r} \int \int p(z') p(z) |z - z'| dz dz' - \varsigma(w) \frac{3a_0^*}{2\pi} (3\pi^2)^{1/3} R_y^* \int p(z)^{4/3} dz + \frac{2\pi e^2}{\epsilon_r} p_{2D} \int p(z) \{|z + l/2| + |z - l/2|\}, \quad (5)$$

where $p(z)$ is the hole density, p_{2D} is the bi-dimensional impurity concentration,

$$m_{ed} = m_{hh} \left[1 + (m_{lh}/m_{hh})^{3/2} \right]^{2/3} = m_{hh} m_a, \\ w = m_{lh}/m_{hh}, \quad a_0^* = \epsilon_r \hbar^2 / e^2 m_{hh}, \quad R_y^* = e^2 / 2\epsilon_r a_0^*,$$

and

$$\varsigma(w) = 2^{-1/3} + (1 - w^2)[w^2(aw + b) + c(4w^3 + 3w^2 + 2w + 1)] \quad [18].$$

Using the variational principle $\delta(E_{TFD} - \mu N) = 0$, with

$$N = \int p(z) dz,$$

we obtain

$$\mu^* = \left[\frac{3\pi^2 p_{au}(z)}{m_a^{3/2}} \right]^{2/3} + V_H^* - \varsigma(w) \frac{2}{\pi} p_{au}^{1/3}(z), \quad (6)$$

where $p_{au}(z) = (a_0^*)^3 p(z)$, $V_H^* = V_H / R_y^*$, and $\mu^* = \mu / R_y^*$. Therefore resolving the quadratic equation for $p_{au}^{1/3}$, and taking into account the physically meaningful solution,

$$p_{au}(z) = \frac{m_a^3 \varsigma^3(w)}{3\pi^5} \left[1 - \sqrt{1 + \frac{\pi^2(\mu^* - V_H^*(z))}{\varsigma^2(w)m_a}} \right]^3. \quad (7)$$

The exchange potential is

$$V_x^*(z) = -\varsigma(w) \frac{2}{\pi} (3\pi^2)^{1/3} p_{au}^{1/3}(z), \quad (8)$$

and using the direct relation between $p_{au}(z)$ and V_H^* , we find

$$V_x^*(z) = -\frac{2\varsigma^2(w)m_a}{\pi^2} \left[1 - \sqrt{1 + \frac{\pi^2(\mu^* - V_H^*(z))}{\varsigma^2(w)m_a}} \right]. \quad (9)$$

We can restrict to $z \leq 0$, since the potential is an even function as in the case of *n*-type DDD quantum wells:

$$\frac{dV_H^*(z)}{dz^2} = -\frac{8m_a^3 \varsigma^3(w)}{3\pi^4} \left[1 - \sqrt{1 + \frac{\pi^2(\mu^* - V_H^*)}{m_a \varsigma^2(w)}} \right] + 8\pi p_{2D} \delta(z + l/2). \quad (10)$$

At this point, it is important to stress that in order to take advantage of the present model, we discard modifications in the form of the Hartree potential due to the exchange effects, while in the level structure and the charge density, these changes are available. Under these conditions the solution for

TABLE I. Paramount features of n -type DDD GaAs quantum wells in the low, intermediate, and high density limit: degeneracy distance l_{deg} , quantum well depth V_0 and degeneracy-energy difference between excited electron states and the basic level $\Delta E_{01} = E_0 - E_1$, $\Delta E_{02} = E_0 - E_2$, etc., the superscripts o and x denote omitting and considering exchange effects respectively (the energy is in meV, the distance in Å and the impurity density in units of 10^{12} cm^{-2}).

| n_{2D} | l_{deg}^o | | | l_{deg}^x | | | ΔE_{01}^o | ΔE_{01}^x | ΔE_{02}^o | ΔE_{02}^x | V_0^o | V_0^x |
|----------|-------------|-------|-------|-------------|-------|-------|-------------------|-------------------|-------------------|-------------------|---------|---------|
| | E_0 | E_1 | E_2 | E_0 | E_1 | E_2 | | | | | | |
| 1 | 400 | 700 | | 360 | 640 | | -18.9 | -22.3 | | | -50.7 | -61.7 |
| 4 | 250 | 400 | 570 | 230 | 280 | 530 | -57.1 | -61.6 | -75.9 | -83.4 | -153.9 | -172.9 |
| 10 | 160 | 250 | 380 | 160 | 240 | 360 | -113.1 | -118.7 | -155.8 | -165.3 | -318.9 | -346.4 |

V_H^* is of the form $1/f^4(z)$, where $f(z)$ is a linear function of z [20],

$$V_H^* - \mu^* = -\frac{\beta^2}{(\beta|z + l/2| + z_{0p})^4}, \quad (11)$$

with $\beta = 2m_a^{3/2}/15\pi$, and $z_{0p} = (\beta^3/\pi p_{2D})^{1/5}$.

Hence the total potential $V^* = V_H^* + V_x^*$ is

$$V^* = -\frac{\beta^2}{(\beta|z + l/2| + z_{0p})^4} - \frac{2\zeta^2(w)m_a}{\pi^2} \times \left[1 - \sqrt{1 + \frac{\pi^2}{\zeta^2(w)m_a} \frac{\beta^2}{(\beta|z + l/2| + z_{0p})^4}} \right] \quad (12)$$

The last equation allows us to avoid a long and troublesome SC calculation. In this way, it is possible to solve two uncoupled Schrödinger-like equations.

3. Results

3.1. n -type DDD GaAs quantum wells

The starting parameters for n -type DDD quantum wells are: $m^* = 0.067$, $\epsilon_r = 12.5$, and $1 \times 10^{12} \leq n_{2D} \leq 1 \times 10^{13} \text{ cm}^{-2}$. In Fig. 1, the potential profile and the square of the wave functions are presented. The impurity density considered is $n_{2D} = 4 \times 10^{12} \text{ cm}^{-2}$, first omitting the many-body effects (Fig. 1a), and after taking them into account (Fig. 1b).

From Fig. 1a and 1b, it is possible to see the relative importance of the exchange effects, since when many-body effects are considered, the depth of the wells increases as well as the energy of electron levels does. In Fig. 2, the electron energy levels are sketched as function of the distance between wells, without (a), and with (b) exchange effects. The impurity concentration in this case is $n_{2D} = 1 \times 10^{12} \text{ cm}^{-2}$. The main features of the energy levels are:

- For $l = 0$ the energy level structure corresponds to a SDD quantum well.
- As the impurity planes get apart, the electron energy levels go down energetically, *i.e.*, the DDD quantum wells behave like a SDD quantum well, with the only

difference that the width of the SDD quantum well increases as interlayer distance of the DDD does. Therefore the wave functions look like the wave functions of a SDD quantum well (Fig. 3).

- The drop of the electron levels halts at a certain distance, depending on the energy level considered, and then the DDD characteristic onset surmounts the SDD ones, as a consequence, the energy levels go up.

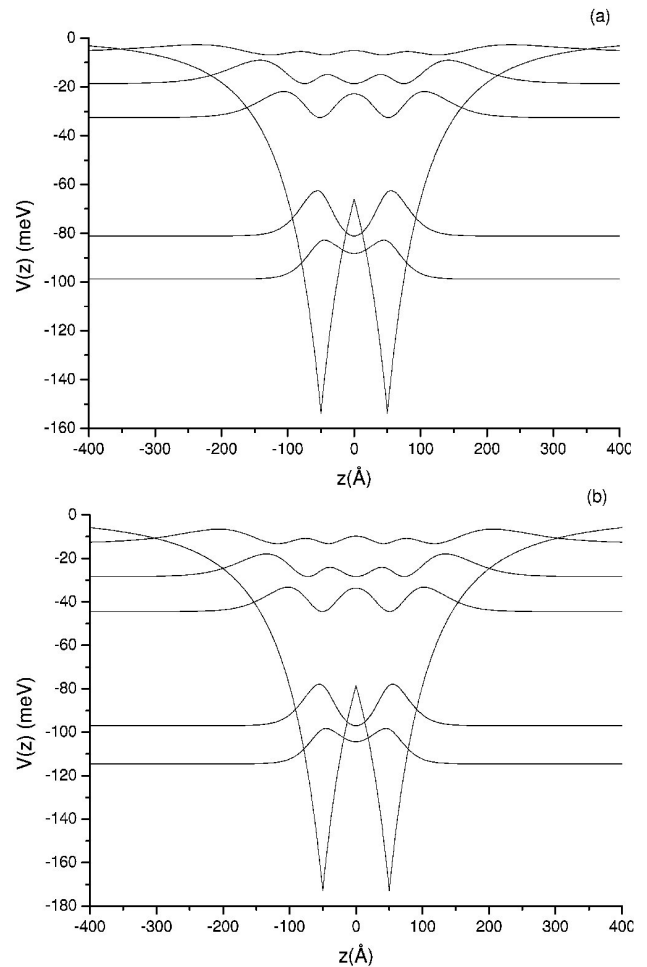


FIGURE 1. Potential profile and electron eigenfunctions for n -type DDD GaAs quantum wells, (a) without and (b) with exchange effects ($n_{2D} = 4 \times 10^{12} \text{ cm}^{-2}$).

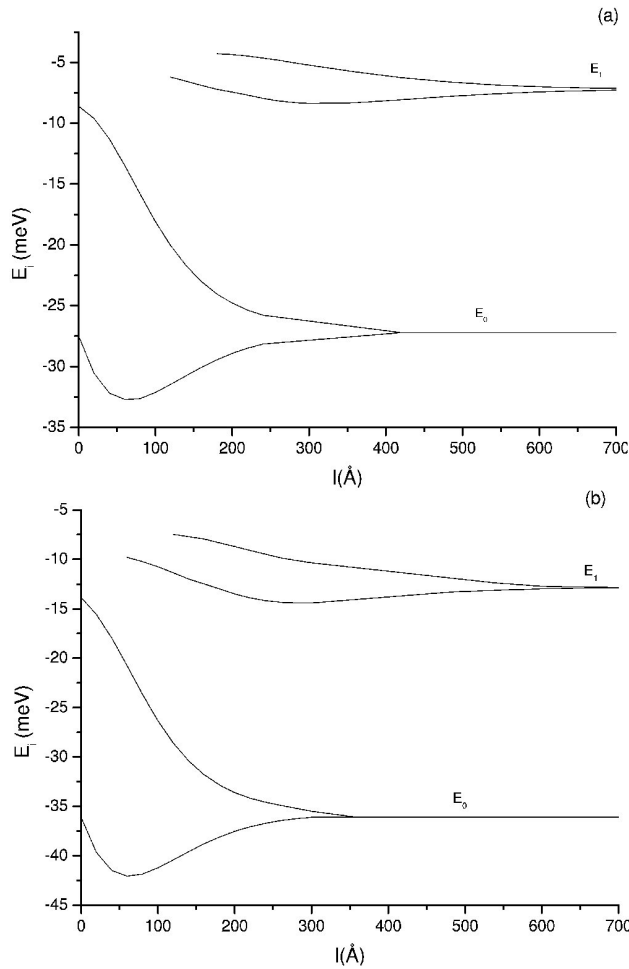


FIGURE 2. Electron states versus the distance between the impurity planes l , for an impurity density of $n_{2D} = 1 \times 10^{12} \text{ cm}^{-2}$, without (a) and with (b) many-body effects.

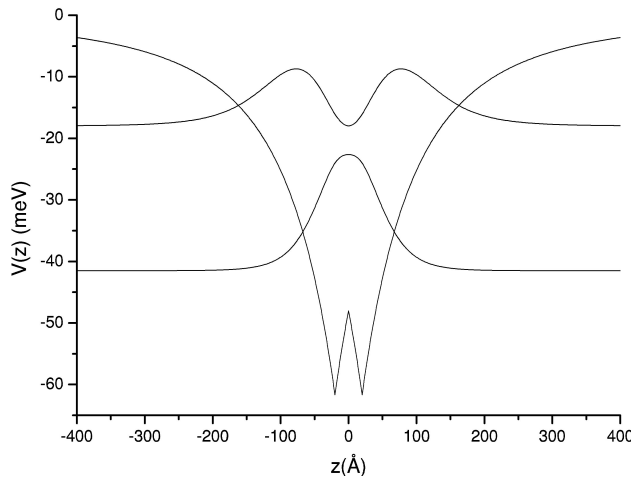


FIGURE 3. SDD behavior of *n*-type DDD quantum wells, the impurity concentration considered is $n_{2D} = 1 \times 10^{12} \text{ cm}^{-2}$ (with exchange effects).

- The energy levels go up, until the degeneration occurs and the level structure again corresponds to a SDD.

In Table I the degeneracy distance (l_{deg}), depth of the quantum wells (V_0), and the degeneracy-energy difference between excited states and the ground level ($E_0 - E_1$, $E_0 - E_2$, etc) are given. We study three different impurity densities with (x) and without (o) exchange effects, in order to analyze the low, intermediate, and high density limits

From Table I we can give a more general description:

1. Increasing the impurity density, the quantum well depth also augments. Thereby it is possible to bound more electron levels.
2. l_{deg} diminishes as the impurity density is increased.
3. The many-body effects are more important in the low density limit.
4. The exchange effects have also relevance in the estimation of the degeneracy-energy difference between the excited states and the ground level.

In Ref. 25 a Si δ -layer with a concentration $n_{2D} = 6.8 \times 10^{12} \text{ cm}^{-2}$ is studied experimentally by infrared excitation. The parity-allowed transitions have energies $E_1 - E_0 = 82.4 \text{ meV}$, and $E_3 - E_0 = 126 \text{ meV}$. Our calculations ($l=0$) give for the same transitions values of 89 and 143 meV, respectively. The subband densities (n_i) measured are 4.7, 1.7, and $0.2 \times 10^{12} \text{ cm}^{-2}$. Our results are $n_0 = 4.3$, $n_1 = 1.7$, and $n_2 = 0.7 \times 10^{12} \text{ cm}^{-2}$. Self-consistent one-electron calculations were performed [26], in which the input parameter was the experimental two-dimensional density of electrons in each level. By $n_{2D} = 3 \times 10^{12} \text{ cm}^{-2}$ the difference between the levels are $E_1 - E_0 = 49 \text{ meV}$, $E_2 - E_0 = 64.3 \text{ meV}$ and $E_3 - E_0 = 71.5 \text{ meV}$. In our calculation ($l=0$) $E_1 - E_0 = 49.8$, $E_2 - E_0 = 67.1$, and $E_3 - E_0 = 76.6 \text{ meV}$. The sub-band densities measured are 2.25, 0.5 and $0.1 \times 10^{12} \text{ cm}^{-2}$. Our outputs ($l=0$) are $n_0 = 1.2$, $n_1 = 0.7$, and $n_2 = 0.2 \times 10^{12} \text{ cm}^{-2}$. Magnetotransport measurements were made in Ref. 27, with $n_{2D} = 3 \times 10^{12} \text{ cm}^{-2}$. The sub-band densities reported are 2.05 and $0.7 \times 10^{12} \text{ cm}^{-2}$. Our results ($l=0$) are 2.1 and $0.7 \times 10^{12} \text{ cm}^{-2}$, respectively. A tunneling experiment was performed by Zachau and coworkers [28]. The basic level obtained is 181 meV ($n_{2D} = 8 \times 10^{12} \text{ cm}^{-2}$). Our calculations give 186 meV ($l=0$). Kim *et al.* [29] measured subband densities, $n_0 = 2.7$ and $n_1 = 0.7$ (in units of 10^{12} cm^{-2}) with $n_{2D} = (3.3 \pm 4) \times 10^{12} \text{ cm}^{-2}$. We obtain ($l=0$) $n_0 = 2.5$ and $n_1 = 0.6$. In all cases considered above our results are with exchange effects.

3.2. *p*-type DDD GaAs quantum wells

In this case, the input parameters are: $m_{hh} = 0.52m_0$, $m_{lh} = 0.087m_0$, $\epsilon_r = 12.5$, and $1 \times 10^{12} \leq p_{2D} \leq 1 \times 10^{13} \text{ cm}^{-2}$. In Fig. 4a and 4b the hole levels are given as function of the interlayer distance l .

TABLE II. The same as in Table I, but now for p -type DDD quantum wells, with $\Delta E_{hh01} = E_{hh0} - E_{hh1}$, $\Delta E_{lh0} = E_{hh0} - E_{lh0}$, $\Delta E_{hh02} = E_{hh0} - E_{hh2}$, etc.

| p_{2D} | l_{deg}^o | | | l_{deg}^x | | | ΔE_{hh01}^o | ΔE_{hh01}^x | ΔE_{lh00}^o | ΔE_{lh00}^x | V_0^o | V_0^x |
|----------|-------------|-----------|-----------|-------------|-----------|-----------|---------------------|---------------------|---------------------|---------------------|---------|---------|
| | E_{hh0} | E_{lh0} | E_{hh1} | E_{hh0} | E_{lh0} | E_{hh1} | | | | | | |
| 1 | 340 | | | 230 | | | | -8.1 | -2.7 | -4.6 | -14.4 | -21.9 |
| 4 | 150 | 440 | 400 | 130 | 350 | 340 | -15.9 | -22.6 | -9.1 | -12.6 | -43.6 | -58.8 |
| 10 | 90 | 300 | 260 | 90 | 270 | 220 | -31.0 | -40.8 | -18.9 | -34.8 | -82.2 | -105.9 |

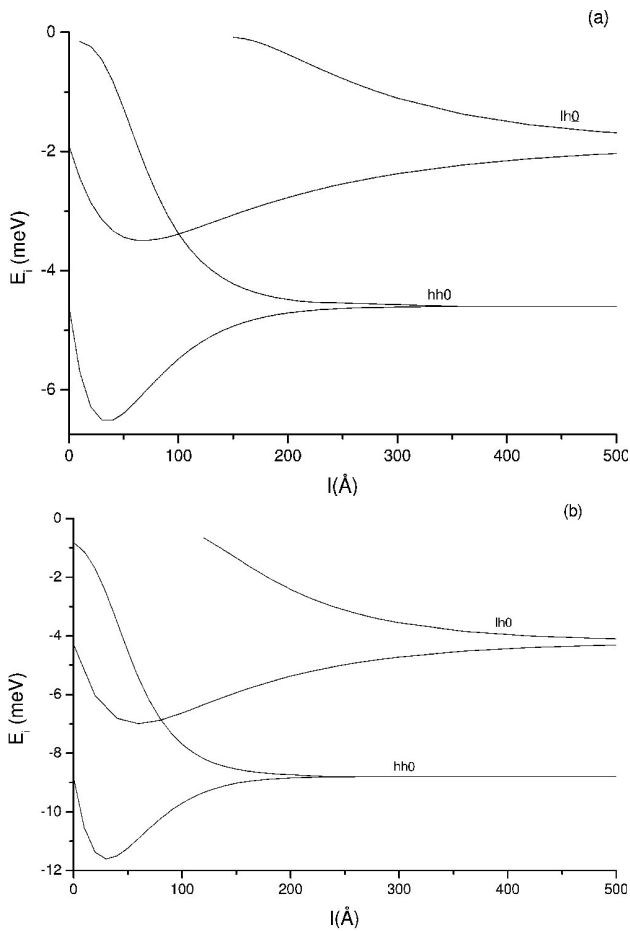


FIGURE 4. Hole subband structure as a function of the interlayer distance between wells, omitting (a) and taking into account (b) exchange effects with $p_{2D} = 1 \times 10^{12} \text{ cm}^{-2}$.

By and large, the behavior of the hole levels in terms of l is the same as in the case of n -type DDD. However, two level ladders appear (hh and lh) and their degeneracy distances are very different as we can see from Figs. 4a and 4b. This depends directly on the effective masses, since the heavy hole mass is greater than the light hole mass, the degeneracy distance diminishes for hh levels as is shown in Figs. 4a and 4b. While for lh levels, the degeneracy distance resembles what happens when the carriers involved are electrons, because the effective mass of lh is approximately the same as for the electrons. Figures 5a and 5b sketch the potential profile and the

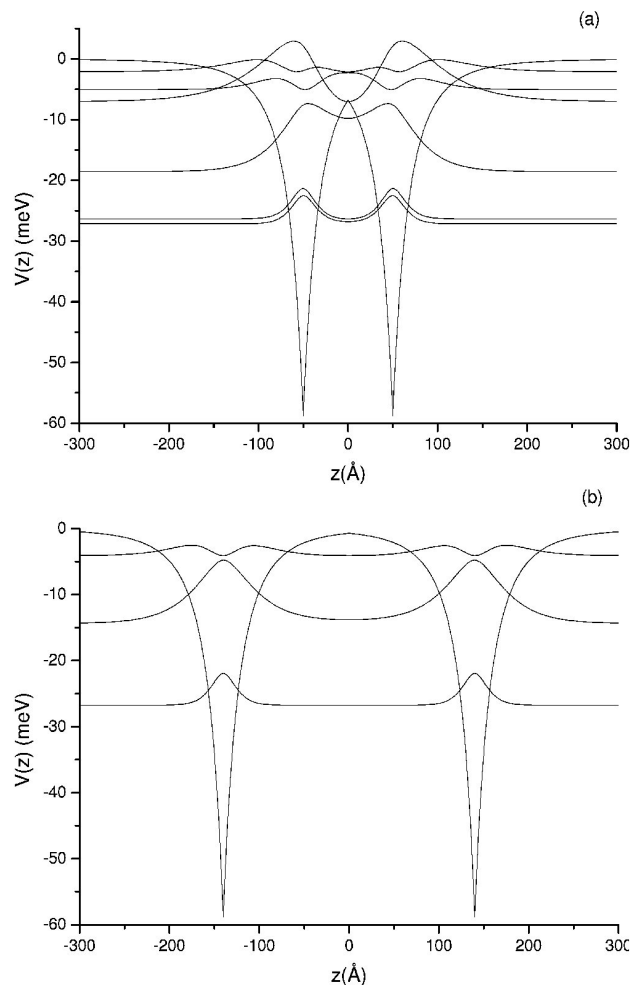


FIGURE 5. Hole eigenfunctions and potential profile, for p -type DDD quantum wells considering exchange effects, for different interlayer distances: (a) 100 Å and (b) 280 Å, with $p_{2D} = 4 \times 10^{12} \text{ cm}^{-2}$.

square of the wave functions for two distances between the impurity planes, (a) 100 Å and (b) 280 Å.

The p -type DDD quantum wells is less deep than the n -type DDD. We can see this comparing Fig. 4a and 4b to Fig. 1b. Besides the hole energy levels are totally degenerated in Fig. 4b with respect to Fig. 4a.

In Table II the main characteristics of p -type DDD are drafted. From this table, we have found that many-body effects are more important in p -type DDD with respect to the

n-type system (see Table I). In the low density limit, a difference of 90 Å between the degeneracy distance, with and without exchange effects is found, for the ground state of *hh*, while in *n*-type system this difference is 40 Å. Increasing the impurity density we can bound more hole levels, predominantly *hh*, because *lh* levels are more de-localized, *i.e.*, the screening and localization is less effective for *lh* (as in the case of electrons) compared with *hh*.

The *p*-type $Al_xGa_{1-x}As/GaAs/Al_xGa_{1-x}As$ quantum wells were grown in Ref. 30, with $p_{2D}=8\times 10^{-2} cm^{-2}$. They reported a subband separation of 36 meV. Although our calculations ($l = 0$) refers to a simpler system, we find an energy difference between first and second *hh* levels of 37 meV. Be δ -doped GaAs quantum wells were grown by Damen and coworkers [31], with $p_{2D} = 6 \times 10^{12} cm^{-2}$. The energy difference between the Fermi level and basic level is 22 meV. We obtain ($l = 0$) an energy difference of about 26 meV. PL spectroscopy study is performed in Ref. 32. Also SC calculations with $p_{2D} = 8 \times 10^{12} cm^{-2}$ were performed. SC results are: $E_{hh0} - E_{lh0} = 15.1$ meV. According to PL spectroscopy measurements this difference is 19 meV. Our calculation ($l = 0$) gives 20 meV. We obtain 14 meV with $p_{2D} = 3 \times 10^{12} cm^{-2}$, whereas the experimental result reported is 11 meV for the same impurity concentration.

Gilinsky and colleagues [33] reported the PL spectrum in *p*-type Be δ -doped GaAs layers for 4×10^{12} , 1.8×10^{13} , and $3.6 \times 10^{12} cm^{-2}$, obtaining $E_{hh0} - E_{lh0} = 8, 20$ and 30 meV, respectively. With the TFD theory ($l = 0$) we obtain 12.5, 35 and 55 meV. The discrepancy, as we can see from the high impurity concentrations, may be due to the impurity spreading.

4. Conclusions

As a final comment, we can say that TF and TFD approximations are very useful tools in the study of semiconductor systems, such as *n*- and *p*-type DDD GaAs quantum wells. These theories permit us to obtain analytical expressions for the potential that represents the corresponding conduction and valence band bending. The electron and hole subband structure calculations reveal the main features of *n*- and *p*-type system. It is shown that exchange effects take more relevance in *p*-type DDD, since the screening is more effective, and the holes are more localized than in the case of electrons. Besides it is important to stress that the TFD theory is only applicable in *p*-type systems. Also our results agree with respect to the experimental data available.

1. C.E.C Wood, G. Metzger, J. Berry, and L.F. Eastman, *J. Appl. Phys.* **51** (1980) 383.
2. K. Ploog, *J. Cryst. Growth* **81** (1987) 304.
3. E.F. Schubert, A. Fischer, and K. Ploog, *IEEE Trans. Electron Devices* **33** (1986) 625.
4. M. Zachau, F. Koch, K. Ploog, P. Roentgen, and H. Beneking, *Solid State Commun.* **59** (1986) 591.
5. K. Köhler, P. Ganser, and M. Maier, *J. Cryst. Growth* **127** (1993) 920.
6. L.M. Gaggero-Sager and R. Pérez-Alvarez, *J. Appl. Phys.* **74** (1995) 4566.
7. E.F. Schubert and K. Ploog, *Jpn. J. Appl. Phys.* **24** (1985) L608.
8. K. Nakagawa, A.A. van Gorkum, and Y. Shiraki, *Appl. Phys. Lett.* **57** (1989) 1869.
9. M. Hirai *et al.*, *J. Cryst. Growth* **150** (1995) 209.
10. D.A. Woolf *et al.*, *J. Cryst. Growth* **150** (1995) 197.
11. T. Iida *et al.*, *J. Cryst. Growth* **150** (1995) 236.
12. L.M. Gaggero-Sager and R. Pérez-Alvarez, *Phys. Stat. Sol. (b)* **197** (1996) 105.
13. G.M. Siphai, P. Enderlein, L.M.R. Scolfaro, and J.R. Leite, *Phys. Rev. B* **53** (1996) 9930.
14. L.M. Gaggero-Sager and R. Pérez-Alvarez, *J. Appl. Phys.* **79** (1996) 3351.
15. N.Y. Li, H.K. Dong, C.W. Tu, and M. Geva, *J. Cryst. Growth* **150** (1995) 246.
16. L.M. Gaggero-Sager, *Modelling and Simulation in Materials Science and Engineering* **9** (2001) 1.
17. L.M. Gaggero-Sager, *Phys. Stat. Sol. (b)* **231** (2002) 243.
18. S.J. Vlaev and L.M. Gaggero-Sager, *Some Contemporary Problems of Condensed Matter Physics* (Nova Science, 2000).
19. G.Q. Hai and N. Studart, *Phys. Rev. B* **52** (1995) 2245.
20. L.M. Gaggero-Sager, J.C. M'Peko, and R. Pérez-Alvarez, *Rev. Mex. Fís.* **47** (2001) 153.
21. E. Ozturk and I. Sokmen, *J. Phys. D* **36** (2003) 2457.
22. X. Zheng, T.K. Carns, K.L. Wang, and B. Wu, *Appl. Phys. Lett.* **62** 504 (1993).
23. H.H. Radamson *et al.*, *Appl. Phys. Lett.* **64** 1842 (1994).
24. V.L. Gurtovoi, V.V. Valyaev, S. Yu. Shapoval, and A.N. Pustovit, *Appl. Phys. Lett.* **72** (1998) 1202.
25. C.A.C. Mendoca *et al.*, *Phys. Rev. B* **48** (1993) 12316.
26. G. Tempel, F. Muller, N. Scharz, F. Koch, G. Weiman, H.P. Zeeindl, and I. Eisele, *Surf. Sci.* **228** (1990) 247.
27. J.C. Egues, A. Barbosa, A.C. Notari, P. Basmaji, L. Ioriatti, E. Ranz, and J. Portal, *J. Appl. Phys.* **70** (1991) 3678.
28. M. Zachau, F. Koch, K. Ploog, P. Roentgen, and H. Beneking, *Solid State Commun.* **59** (1986) 591.
29. T.W. Kim, K.-H. Yoo, K.-S. Lee, Y. Kim, S.-K. Min, S.S. Yom, and S.J. Lee, *J. Appl. Phys.* **76** (1994) 2863.
30. J. Wagner, A. Ruiz, and K. Ploog, *Phys. Rev. B* **43** (1991) 12134.
31. T.C. Damen *et al.*, *Appl. Phys. Lett.* **67** (1995) 515.
32. D. Richards *et al.*, *Phys. Rev. B* **47** (1993) 9629.
33. A.M. Gilinsky *et al.*, *Superlatt. Microstruct.* **10** (1991) 399.